Korean J Physiol Pharmacol 2017;21(4):371-376
https://doi.org/10.4196/kjpp.2017.21.4.371

KJPP

Original Article

Reactive oxygen species increase neuronal excitability via activation of nonspecific cation channel in rat medullary dorsal horn neurons

Hae In Lee[1], Byung Rim Park[2], and Sang Woo Chun[3,*]

[1]Department of Dental Hygiene, Gwangyang Health Science University, Gwangyang 57764, [2]Department of Physiology, College of Medicine, Wonkwang University, Iksan 54538, [3]Department of Oral Physiology, College of Dentistry, Wonkwang University, Iksan 54538, Korea

ARTICLE INFO

Received December 27, 2016
Revised March 10, 2017
Accepted March 20, 2017

***Correspondence**
Sang-Woo Chun
E-mail: physio1@wonkwang.ac.kr

Key Words
Nonspecific cation channel
Orofacial pain
Reactive oxygen species
Xanthine oxidase

ABSTRACT The caudal subnucleus of the spinal trigeminal nucleus (medullary dorsal horn; MDH) receives direct inputs from small diameter primary afferent fibers that predominantly transmit nociceptive information in the orofacial region. Recent studies indicate that reactive oxygen species (ROS) is involved in persistent pain, primarily through spinal mechanisms. In this study, we aimed to investigate the role of xanthine/xanthine oxidase (X/XO) system, a known generator of superoxide anion ($O_2^{\cdot-}$), on membrane excitability in the rat MDH neurons. For this, we used patch clamp recording and confocal imaging. An application of X/XO (300 μM/30 mU) induced membrane depolarization and inward currents. When slices were pretreated with ROS scavengers, such as phenyl N-tert-butylnitrone (PBN), superoxide dismutase (SOD), and catalase, X/XO-induced responses decreased. Fluorescence intensity in the DCF-DA and DHE-loaded MDH cells increased on the application of X/XO. An anion channel blocker, 4,4-diisothiocyanatostilbene-2,2-disulfonic acid (DIDS), significantly decreased X/XO-induced depolarization. X/XO elicited an inward current associated with a linear current-voltage relationship that reversed near –40 mV. X/XO-induced depolarization reduced in the presence of La^{3+}, a nonselective cation channel (NSCC) blocker, and by lowering the external sodium concentration, indicating that membrane depolarization and inward current are induced by influx of Na^+ ions. In conclusion, X/XO-induced ROS modulate the membrane excitability of MDH neurons, which was related to the activation of NSCC.

INTRODUCTION

The subnucleus caudalis of the spinal trigeminal sensory nucleus is frequently termed the medullary dorsal horn (MDH) owing to its anatomical and physiological similarity with the spinal dorsal horn. The small myelinated Aδ-fiber and unmyelinated C-fiber enter the spinal trigeminal tract and terminate primarily in lamina I and II of the MDH. Therefore, the MDH is known as the center for processing pain from the craniofacial area, and for transmitting the integrated signals to the upper brain [1,2].

Reactive oxygen species (ROS), such as superoxide anion ($O_2^{\cdot-}$), hydrogen peroxide (H_2O_2), and nitric oxide (NO) contribute to the increase of pain hypersensitivity during persistent pain [3,4]. Recently, Wang et al. reported that application of superoxide dismutase (SOD), which breaks down $O_2^{\cdot-}$, prevents the development of inflammation and hyperalgesia following the injection of an inflammatory agent into the paw [5]. Other studies have reported an increased ROS production in the dorsal horn following spinal cord injury (SCI), which was attenuated

Author contributions: H.I.L. performed patch clamp recording and confocal imaging experiments. H.I.L. and S.W.C. wrote the manuscript. B.R.P. performed the interpretation of data and revising the manuscript. S.W.C. supervised the study.

by treatment with ROS scavengers such as phenyl N-tert-butylnitrone (PBN) or 4-hydroxy-2,2,6,6-tetramethylpiperidine-1-oxyl (TEMPOL) [6,7]. Furthermore, ROS accumulation was observed primarily in the mitochondria of dorsal horn neurons after capsaicin treatment [8]. These results suggest that $O_2^{\cdot-}$ participates in the nociceptive signaling cascade.

Increased production of ROS has been shown to affect membrane excitability related to the activity of ion channels. For example, voltage-dependent Na^+, K^+, and Ca^{2+} channels, Ca^{2+}-activated K^+ channels, and K_{ATP} channels have been identified as targets for ROS [9,10]. In addition, H_2O_2 induced membrane depolarization and increased excitability in medium spiny neurons via activation of TRP channels [11]. Moreover, NO, induced by an application of sodium nitroprusside, have been reported to influence the membrane potential of spinal substantia gelatinosa neurons via modification of various K^+ channels and nonspecific cation channels (NSCC) [12].

Xanthine oxidase (XO) is an important enzymatic source of $O_2^{\cdot-}$. This enzyme catalyzes the conversion of hypoxanthine and xanthine to uric acid, which produces an enormous amount of $O_2^{\cdot-}$ [13]. XO levels have been reported to increase in a model of neuropathic pain [14], and increased XO activity and $O_2^{\cdot-}$ production has been suggested to play a role in the development of pain [15]. However, the effects of $O_2^{\cdot-}$ generated by XO on the excitability of MDH neurons and the underlying ionic mechanisms have not been elucidated.

In this study, we investigated whether ROS derived from XO contribute to pain transmission by affecting the membrane potential and the ionic current of MDH neurons. For that, we used patch-clamp recordings from transverse slices of the spinal trigeminal nucleus. To our knowledge, this is the first study in which the effects of $O_2^{\cdot-}$ generated by the X/XO system on membrane excitability in MDH neurons were investigated.

METHODS

Brain slice preparation

Sprague-Dawley rats (13~18 days old) were anesthetized with ether. The procedures were approved by the University of Wonkwang Committee on Ethics in the Care and Use of Laboratory Animals (WKU09-076). Rats were decapitated and the brain stem was rapidly removed and placed in an ice-cold solution at 0~4°C. The brain stem was glued to the stage of a vibrating microslicer (752M, Campden Instruments, Loughborough, UK) and cut into 150~350 μm-thick slices. Slices were subsequently incubated at 32°C for at least 1 h with 95% O_2 and 5% CO_2. Then, slices were transferred to a recording chamber mounted on an upright microscope.

Solutions and drugs

The dissecting solution used for the preparation of brain slices was composed of: sucrose (252 mM), KCl (2.5 mM), $CaCl_2$ (0.1 mM), $MgCl_2$ (2 mM), Glucose (10 mM), $NaHCO_3$ (26 mM), and NaH_2PO_4 (1.25 mM). The extracellular fluid used for the patch-clamp recording contained: NaCl (117 mM), KCl (3.6 mM), $CaCl_2$ (2.5 mM), $MgCl_2$ (1.2 mM), NaH_2PO_4 (1.2 mM), $NaHCO_3$ (25 mM), and glucose (11 mM). It was continually aerated with 95% O_2 and 5% CO_2, which maintained the pH at approximately 7.4. The pipette (internal) solution contained: K-Glu (150 mM), HEPES (10 mM), KCl (5 mM), EGTA (0.1 mM), Mg-ATP (2 mM), and NaGTP (0.3 mM). The pH was adjusted to 7.2 using KOH. In low Na^+ external solution, equimolar choline-Cl replaced NaCl. The following reagents were obtained from Sigma-Aldrich (St. Louis, MO, USA): X, XO, PBN, catalase, superoxide dismutase (SOD), 4,4-diisothiocyanatostilbene-2,2-disulfonic acid (DIDS). Dihydroethidium (DHE) and 2',7'-dichlorofluorescin diacetate (DCF-DA) were obtained from Molecular Probes (Eugene, OR, USA).

Patch-clamp recording

Microelectrodes were prepared from capillary glass tubes (TW150-3, WPI, USA) using a microelectrode pipette puller (PP830, Narishige, Japan). Patch pipettes, filled with the pipette solutions, were used at a resistance ranging from 6 to 8 MΩ. The MDH of the spinal trigeminal nucleus was viewed using an upright microscope (BX50WI, Olympus, Japan). Membrane potentials and currents were recorded using an Axopatch 200B amplifier (Axon Instruments, USA) that was connected to a computer using an A/D converter (Digidata 1322A, Axon Instruments, USA). Membrane potential recording and data analyses were performed using the pClamp software (version 9.0, Axon Instruments, USA). Generated currents were filtered with a low-pass 8-pole Bessel filter at 2 kHz. All experiments were performed at room temperature (22±1°C).

Fluorescence imaging

The slices were loaded with fluorescence dyes including DCF-DA and DHE for 10~30 min at 30°C. The slices were examined on an inverted fluorescence microscope (x200; LSM 510, Carl Zeiss, Germany). Confocal laser scanning microscopy was used with two lasers, i.e. an argon ion laser emitting at 488 nm and a HeNe laser emitting at 543 nm to excite FITC and Cy3, respectively. A time series was used to record images every 30 s. The fluorescence intensity was analyzed in predefined a region of interest (ROI).

Data analysis

Differences in drug effects were analyzed using *t*-test and

were considered significant when p<0.05 was obtained. Data are expressed as mean±standard error of the mean (SEM).

RESULTS

Effects of X/XO on the membrane excitability in MDH neurons

We examined whether the xanthine plus xanthine oxidase (X/XO) affects membrane excitability in MDH neurons. During current-clamp recording, the administration of X/XO (300 μM/30 mU) for 5 min induced a reversible membrane depolarization (5.6±0.3 mV, n=95). When an MDH neuron was clamped at a holding potential of –60 mV in voltage clamp recording, X/XO induced an inward current (–8.2±0.6 pA, n=20). To determine whether X/XO-induced changes were due to the release of ROS, MDH neurons were pretreated with ROS scavengers, including PBN (2 mM), SOD (50 U), and catalase (1000 U) plus SOD, prior to the application of X/XO. X/XO-induced depolarization significantly reduced in the presence of the ROS scavengers, such as PBN (3.1±0.5 mV, n=7, p<0.05), SOD (2.9±0.4 mV, n=7, p<0.01), and catalase plus SOD (2.1±0.3 mV, n=10, p<0.01) (Fig. 1). These results suggest that ROS are released by X/XO, which in turn induces changes in the membrane excitability of MDH neurons.

Furthermore, intracellular ROS generation by X/XO was assessed using DCF-DA and DHE. The intracellular fluorescence intensity in DCF-DA- and DHE-loaded cells increased during perfusion of X/XO for 5 min (151.8±6.2%, n=8, p<0.001, and 139.2±7.9%, n=8, p<0.001), which was inhibited by the ROS scavenger PBN (120.6±7.5%, n=5, p<0.01, and 110.0±3.4%, n=5, p<0.01) (Fig. 2).

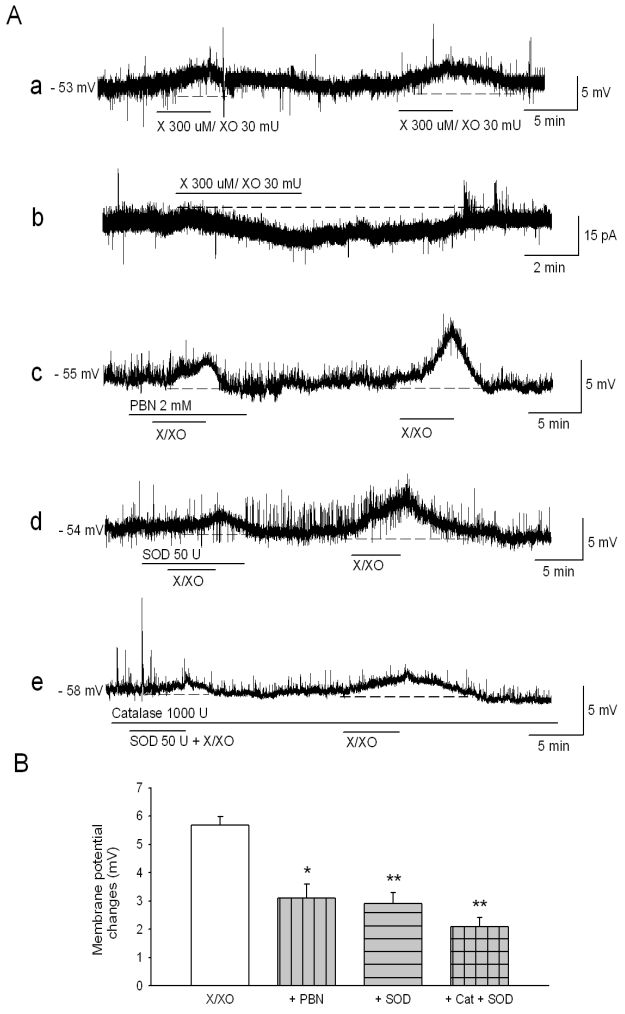

Fig. 1. X/XO-induced membrane depolarization is attenuated by pretreatment with ROS scavengers. The X/XO elicited a depolarization (Aa) and inward current (Ab), repeatedly. The X/XO-induced depolarization was significantly suppressed by pretreatment with PBN (Ac), SOD (Ad), and SOD+catalase (Ae). (B) Summary data obtained under the control condition of X/XO-induced depolarization and pretreatment with antioxidants. **Values are significantly different from the X/XO by independent *t*-test (p<0.01). *p<0.05. Means±SEM.

The ionic mechanism underlying X/XO-induced responses

The addition of X/XO is known to initially generate $O_2^{\cdot-}$, which has a low permeability in the membrane [16]. Moreover, extracellular $O_2^{\cdot-}$ can enter the cell through the anion channel and can participate in intracellular signaling either directly or by binding to other substances [17]. To confirm whether indeed X/XO-derived $O_2^{\cdot-}$ enters the cell via anion channels, we applied

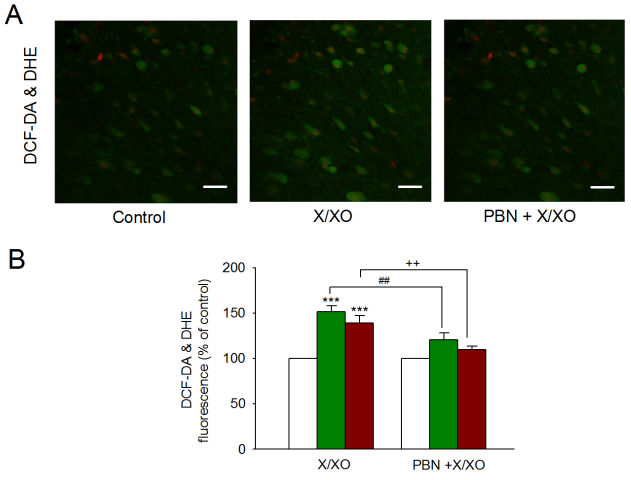

Fig. 2. X/XO-induced increase of the fluorescence intensity is attenuated by pretreatment with PBN. (A) Fluorescence intensity in the DCF-DA (green) and DHE-loaded (red) MDH cells increased on the application of X/XO (center); while PBN (right) prevented the X/XO-induced fluorescence increase (scale bars: 20 μm). (B) The results were quantitatively analyzed as percent units of DCF-DA and DHE fluorescence of the control. ***Values are significantly different from the control by paired *t*-test (p<0.001). ##Values are significantly different between X/XO and PBN+X/XO in DCF-DA fluorescence by paired *t*-test (p<0.01). ++Values are significantly different between X/XO and PBN+X/XO in DHE fluorescence (p<0.01). Means±SEM.

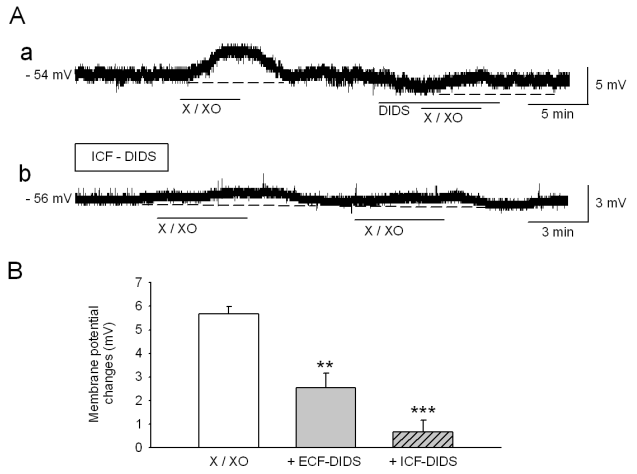

Fig. 3. The changes of neuronal excitability by X/XO are related to the chloride channel. The X/XO-induced depolarization decreased by DIDS (300 μM), an inhibitor of chloride channel within bath (Aa) or pipette solution (Ab). (B) Bar graph showing the effects of DIDS on X/XO-induced depolarization. ***Values are significantly different from the X/XO by independent t-test (p<0.001). **p<0.01. Means±SEM.

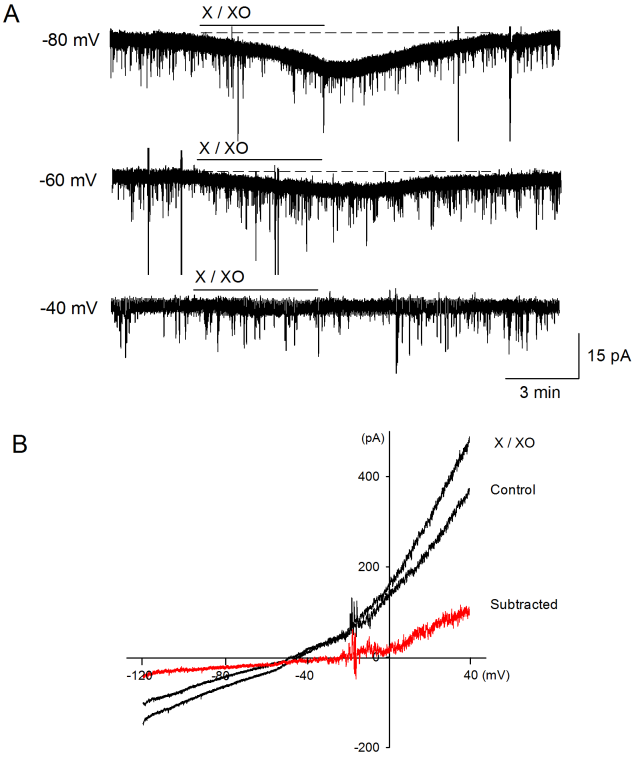

Fig. 4. X/XO-induced current is consistent with the opening of a nonselective cation channel. (A) X/XO-induced current from different holding potentials. At a holding potential of –40 mV, X/XO-induced current does not appeared. (B) In normal ECF solution, the current during a ramp from –120 to 40 mV increased on application of X/XO. Subtracted current (X/XO minus control) is reversed near –40 mV.

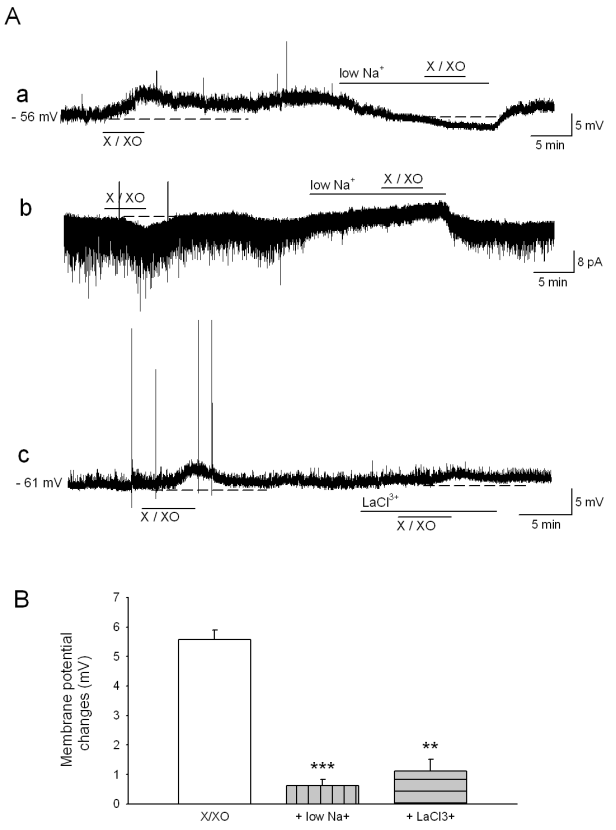

Fig. 5. X/XO-induced responses are involved in the influx of Na^+ ions. (A) In low Na^+ solution, X/XO-induced depolarization (a) and inward current (b) significantly decreased. (Ac) In La^{3+}, a nonspecific cation channel blocker, containing solution, X/XO-induced depolarization decreased. (B) Bar graph showed that the effects of low Na^+ and La^{3+} on X/XO-induced depolarization. ***Values are significantly different from the X/XO by independent *t*-test (p<0.001). **p<0.01. Means±SEM.

DIDS, an anion channel blocker. The application of DIDS (300 μM) within the bath (external) or the pipette (internal) solution significantly inhibited depolarization by X/XO (2.5±0.6 mV, n=11, p<0.01 and 0.6±0.5 mV, n=7, p<0.001, respectively) (Fig. 3). These results suggest that $O_2^{\cdot-}$ moves from the extracellular into the intracellular space through anion channels, and subsequently contributes to intracellular signaling.

We next investigated which ions generate X/XO-induced depolarization and inward currents. In the voltage clamp condition, X/XO was applied at different holding potentials (–80 mV, –60 mV and –40 mV). X/XO-induced inward currents reduced at the depolarized holding potential. At a holding potential of –40 mV, no currents occurred. In addition, when a ramp pulse ranging from –120 to +40 mV was applied, the subtracted current (X/XO minus control) was reversed at a more positive than –40 mV (Fig. 4). Therefore, these findings suggest that the X/XO-induced current transports K^+ as well as Na^+. Furthermore, X/XO-induced depolarization is significantly reduced in the presence of the external low Na^+ solution and an

 https://doi.org/10.4196/kjpp.2017.21.4.371

NSCC blocker, La^{3+} (100 μM) (0.6±0.3 mV, n=8, p<0.001 and 1.1±0.5 mV, n=13, p<0.01, respectively) (Fig. 5). These results indicate that membrane depolarization and inward currents are induced by influx of Na^+ ions via NSCC.

DISCUSSION

ROS are possibly involved in the pathophysiology of diabetes, cancer, neurodegenerative diseases, and aging [18-20]. However, recent studies have shown that physiological concentrations of ROS mediate reversible regulatory processes and signaling [21]. The contribution of ROS to nociceptive processing has been revealed by several studies. For example, ROS are produced into the spinal trigeminal nucleus during a persistent facial pain induced by a subcutaneous injection of formalin. Moreover, decreased superoxide dismutase (SOD) activity was associated with an increased pain behavior [22], suggesting that elevated ROS levels in the spinal trigeminal nucleus are sufficient to induce pain.

There are various sources to produce ROS during pain processing. For example, ROS can be generated from mitochondria (complexes I and III of the electron transport chain), xanthine oxidase, cyclooxygenases, and nicotinamide adenine dinucleotide phosphate (NADPH) oxidases [23]. In this study, X/XO was applied in MDH neurons in order to induce a ROS generation. During the current-clamp recording, administration of X/XO for 5 min induced membrane depolarization, which was significantly reduced by ROS scavengers, such as PBN, SOD, and catalase (Fig. 1). In addition, ROS generation was confirmed by DCF-DA and DHE fluorescence imaging in slices containing MDH neurons (Fig. 2). These results suggest that ROS were produced following the application of X/XO, which in turn induced changes in membrane excitability of the MDH neurons.

Laser confocal microscopy has been used to investigate the role of ROS in cellular signaling, and several fluorescent proves have been designed to detect ROS that are associated with cellular oxidative stress. For example, DCF-DA is a relatively nonselective prove that reacts with free radical in the cytoplasm, nucleus, and mitochondria [24]. It diffuses passively into cells, where the acetate group is cleaved by intracellular esterase, and DCF remains inside the cells to develop fluorescence. DCF-DA is reported to detect not only H_2O_2, but also $O_2^{\cdot-}$, hydroxyl radical (·OH), NO, and peroxynitrite (ONOO-) [25]. On the other hand, DHE prove is very sensitive to $O_2^{\cdot-}$. When it meets $O_2^{\cdot-}$, it is oxidized to the fluorescent product ethidium bromide. However, it has very low sensitivity to H_2O_2 and does not react well with ·OH or $ONOO^-$ [26].

The $O_2^{\cdot-}$ has a low permeability in the membrane [27]. Additionally, since $O_2^{\cdot-}$ is not only a free radical but also an anion, it is possible that its effect in the cell can occur by influx through the chloride channel [17]. Several previous studies have provided evidence for $O_2^{\cdot-}$ transport through anion channels, which could be effectively blocked by DIDS [28,29]. Moreover, the DIDS is also known to block $O_2^{\cdot-}$ release from the mitochondria into the cytosol [30]. A voltage-dependent anion channel (VDAC) located in the mitochondrial outer membrane plays the role of a pore that releases mitochondria-generated $O_2^{\cdot-}$ to the cytosol [31]. In the present study, pretreatment of DIDS within both bath and pipette solution significantly inhibited X/XO-induced depolarization (Fig. 3). These findings indicate that X/XO-induced $O_2^{\cdot-}$ transfer from the extracellular into the intracellular space via anion channels. Therefore, $O_2^{\cdot-}$ contributes to the signaling intracellular pathway.

Depolarization of the plasma membrane was observed on the addition of oxidizing agents such as H_2O_2, t-BHP, or nitric oxide. This effect can be associated with activation of a NSCC, which is characterized by a linear I-V relationship [12,32]. In our experiments, X/XO elicited an inward current associated with a voltage-independent linear current-voltage relationship that reversed near −40 mV (Fig. 4). Hung and Magoski [33] reported that the approximately −40 mV reversal potential suggests the involvement of voltage-independent NSCC. A reversal potential between −45 and +20 mV is dependent upon a varying degree of cation selectivity [34]. Moreover, X/XO-induced depolarization significantly reduced in the presence of low Na^+ solution and La^{3+}, an NSCC blocker (Fig. 5). These results indicate that X/XO-induced membrane depolarization and inward currents are induced by influx of Na^+ ions through the NSCC.

In summary, the present study presents evidence that $O_2^{\cdot-}$ flux across the plasma membrane occurs through chloride channels. Moreover, membrane depolarization and inward current are induced by influx of Na^+ ions via NSCC. These are essential steps for modulating the membrane excitability by $O_2^{\cdot-}$, which generated by the X/XO system in spinal trigeminal MDH neurons. In conclusion, these results suggest that $O_2^{\cdot-}$, in addition to its role as a toxin, can also be considered a signaling molecule for pain transmission.

ACKNOWLEDGEMENTS

This paper was supported by Wonkwang University in 2015.

CONFLICTS OF INTEREST

The authors declare no conflicts of interest.

REFERENCES

1. Dubner R, Bennett GJ. Spinal and trigeminal mechanisms of nociception. *Annu Rev Neurosci.* 1983;6:381-418.

2. Sessle BJ. Acute and chronic craniofacial pain: brainstem mechanisms of nociceptive transmission and neuroplasticity, and their clinical correlates. *Crit Rev Oral Biol Med.* 2000;11:57-91.
3. Meller ST, Cummings CP, Traub RJ, Gebhart GF. The role of nitric oxide in the development and maintenance of the hyperalgesia produced by intraplantar injection of carrageenan in the rat. *Neuroscience*. 1994;60:367-374.
4. Liu D, Liu J, Sun D, Wen J. The time course of hydroxyl radical formation following spinal cord injury: the possible role of the iron-catalyzed Haber-Weiss reaction. *J Neurotrauma.* 2004;21:805-816.
5. Wang ZQ, Porreca F, Cuzzocrea S, Galen K, Lightfoot R, Masini E, Muscoli C, Mollace V, Ndengele M, Ischiropoulos H, Salvemini D. A newly identified role for superoxide in inflammatory pain. *J Pharmacol Exp Ther.* 2004;309:869-878.
6. Kim HY, Wang J, Lu Y, Chung JM, Chung K. Superoxide signaling in pain is independent of nitric oxide signaling. *Neuroreport.* 2009;20:1424-1428.
7. Gwak YS, Hassler SE, Hulsebosch CE. Reactive oxygen species contribute to neuropathic pain and locomotor dysfunction via activation of CamKII in remote segments following spinal cord contusion injury in rats. *Pain.* 2013;154:1699-1708.
8. Schwartz ES, Lee I, Chung K, Chung JM. Oxidative stress in the spinal cord is an important contributor in capsaicin-induced mechanical secondary hyperalgesia in mice. *Pain.* 2008;138:514-524.
9. Kourie JI. Interaction of reactive oxygen species with ion transport mechanisms. *Am J Physiol.* 1998;275:C1-24.
10. Hool LC. Reactive oxygen species in cardiac signalling: from mitochondria to plasma membrane ion channels. *Clin Exp Pharmacol Physiol.* 2006;33:146-151.
11. Bao L, Avshalumov MV, Rice ME. Partial mitochondrial inhibition causes striatal dopamine release suppression and medium spiny neuron depolarization via H2O2 elevation, not ATP depletion. *J Neurosci.* 2005;25:10029-10040.
12. Park AR, Lee HI, Semjid D, Kim DK, Chun SW. Dual effect of exogenous nitric oxide on neuronal excitability in rat substantia gelatinosa neurons. *Neural Plast.* 2014. doi: 10.1155/2014/628531.
13. Herken H, Gurel A, Selek S, Armutcu F, Ozen ME, Bulut M, Kap O, Yumru M, Savas HA, Akyol O. Adenosine deaminase, nitric oxide, superoxide dismutase, and xanthine oxidase in patients with major depression: impact of antidepressant treatment. *Arch Med Res.* 2007;38:247-252.
14. Khalil Z, Khodr B. A role for free radicals and nitric oxide in delayed recovery in aged rats with chronic constriction nerve injury. *Free Radic Biol Med.* 2001;31:430-439.
15. Kwak KH, Han CG, Lee SH, Jeon Y, Park SS, Kim SO, Baek WY, Hong JG, Lim DG. Reactive oxygen species in rats with chronic post-ischemia pain. *Acta Anaesthesiol Scand.* 2009;53:648-656.
16. Sato E, Mokudai T, Niwano Y, Kohno M. Kinetic analysis of reactive oxygen species generated by the in vitro reconstituted NADPH oxidase and xanthine oxidase systems. *J Biochem.* 2011;150:173-181.
17. Brzezinska AK, Lohr N, Chilian WM. Electrophysiological effects of $O_2^{\cdot-}$ on the plasma membrane in vascular endothelial cells. *Am J Physiol Heart Circ Physiol.* 2005;289:H2379-2386.
18. Callaghan MJ, Ceradini DJ, Gurtner GC. Hyperglycemia-induced reactive oxygen species and impaired endothelial progenitor cell function. *Antioxid Redox Signal.* 2005;7:1476-1482.
19. Kregel KC, Zhang HJ. An integrated view of oxidative stress in aging: basic mechanisms, functional effects, and pathological considerations. *Am J Physiol Regul Integr Comp Physiol.* 2007;292:R18-36.
20. Loffredo L, Marcoccia A, Pignatelli P, Andreozzi P, Borgia MC, Cangemi R, Chiarotti F, Violi F. Oxidative-stress-mediated arterial dysfunction in patients with peripheral arterial disease. *Eur Heart J.* 2007;28:608-612.
21. Sorce S, Krause KH. NOX enzymes in the central nervous system: from signaling to disease. *Antioxid Redox Signal.* 2009;11:2481-2504.
22. Viggiano A, Monda M, Viggiano A, Viggiano D, Viggiano E, Chiefari M, Aurilio C, De Luca B. Trigeminal pain transmission requires reactive oxygen species production. *Brain Res.* 2005;1050:72-78.
23. Kallenborn-Gerhardt W, Schröder K, Geisslinger G, Schmidtko A. NOXious signaling in pain processing. *Pharmacol Ther.* 2013;137:309-317.
24. Shanker G, Aschner JL, Syversen T, Aschner M. Free radical formation in cerebral cortical astrocytes in culture induced by methylmercury. *Brain Res Mol Brain Res.* 2004;128:48-57.
25. Hempel SL, Buettner GR, O'Malley YQ, Wessels DA, Flaherty DM. Dihydrofluorescein diacetate is superior for detecting intracellular oxidants: comparison with 2',7'-dichlorodihydrofluor escein diacetate, 5(and 6)-carboxy-2',7'-dichlorodihydrofluorescein diacetate, and dihydrorhodamine 123. *Free Radic Biol Med.* 1999;27:146-159.
26. Bindokas VP, Jordán J, Lee CC, Miller RJ. Superoxide production in rat hippocampal neurons: selective imaging with hydroethidine. *J Neurosci.* 1996;16:1324-1336.
27. Sgherri CLM, Pinzino C, Navari-Izzo F. Sunflower seedlings subjected to increasing stress by water deficit: Changes in $O_2^{\cdot-}$ production related to the composition of thylakoid membranes. *Physiol Plant.* 1996;96:446-452.
28. Lynch RE, Fridovich I. Permeation of the erythrocyte stroma by superoxide radical. *J Biol Chem.* 1978;253:4697-4699.
29. Ikebuchi Y, Masumoto N, Tasaka K, Koike K, Kasahara K, Miyake A, Tanizawa O. Superoxide anion increases intracellular pH, intracellular free calcium, and arachidonate release in human amnion cells. *J Biol Chem.* 1991;266:13233-13237.
30. Han D, Antunes F, Canali R, Rettori D, Cadenas E. Voltage-dependent anion channels control the release of the superoxide anion from mitochondria to cytosol. *J Biol Chem.* 2003;278:5557-5563.
31. Granville DJ, Gottlieb RA. The mitochondrial voltage-dependent anion channel (VDAC) as a therapeutic target for initiating cell death. *Curr Med Chem.* 2003;10:1527-1533.
32. Koliwad SK, Kunze DL, Elliott SJ. Oxidant stress activates a non-selective cation channel responsible for membrane depolarization in calf vascular endothelial cells. *J Physiol.* 1996;491:1-12.
33. Hung AY, Magoski NS. Activity-dependent initiation of a prolonged depolarization in aplysia bag cell neurons: role for a cation channel. *J Neurophysiol.* 2007;97:2465-2479.
34. Partridge LD, Müller TH, Swandulla D. Calcium-activated non-selective channels in the nervous system. *Brain Res Brain Res Rev.* 1994;19:319-325.